Velocimetrie par Images de Particules

M. Stanislas,

Ecole Centrale de Lille

Laboratoire de Mécanique de Lille

CENTRALE LILLE

LABORATOIRE de MECANIQUE de LILLE UMR CNRS 8107

E.C. LILLE E.N.S.A.M. U.S.T.L.

Vocabulaire

PIV Standard : 2D2C

SPIV : 2D3C

Tomo PIV : 3D3C

Micro PIV

Long range Micro PIV

HR PIV

TR PIV

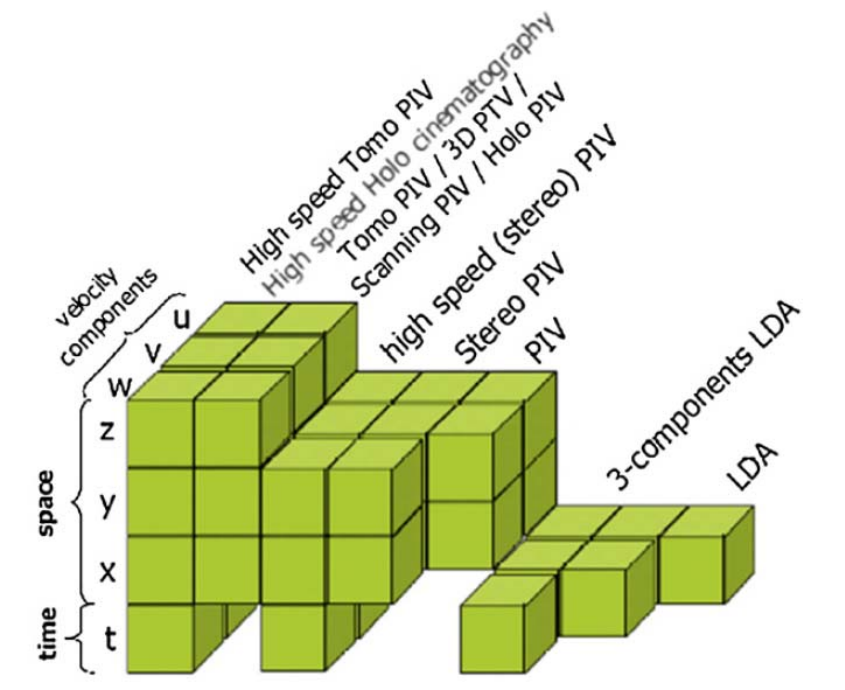

TOC

- **Précision**
- **Résolution spatiale**
- **3D3C**
- **TR PIV**

Paramètres importants

- Taille des images de particules
- Qualité des images de particules
- Concentration en particules
- Calibration (correction)

Algorithmes

- **Multipasses/Multigrilles**
- **Déformation de l’image**
- **Flow Optic**
- **Correlation d’ensemble**
- **PTV**

Précision

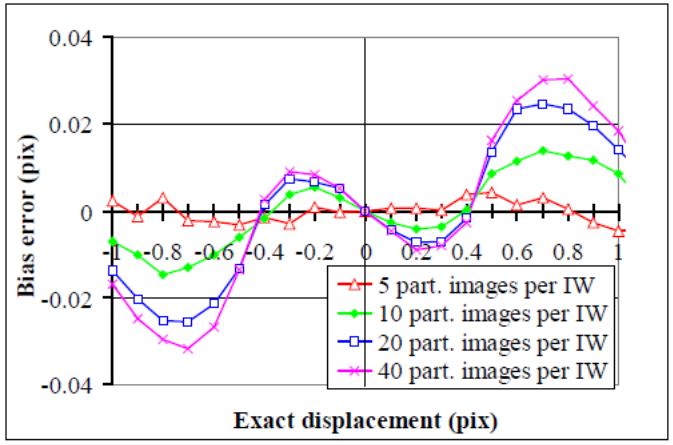

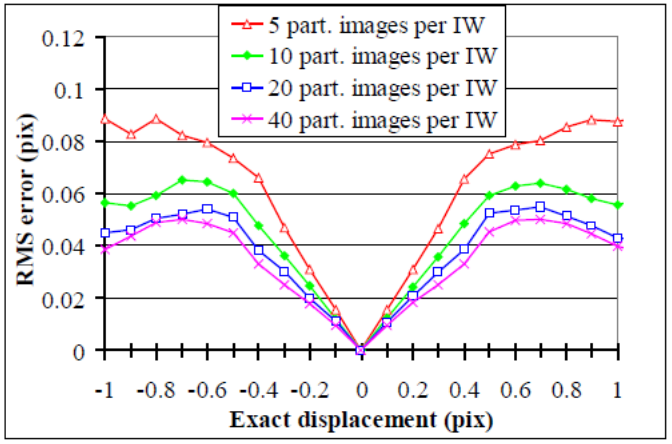

Influence de la concentration

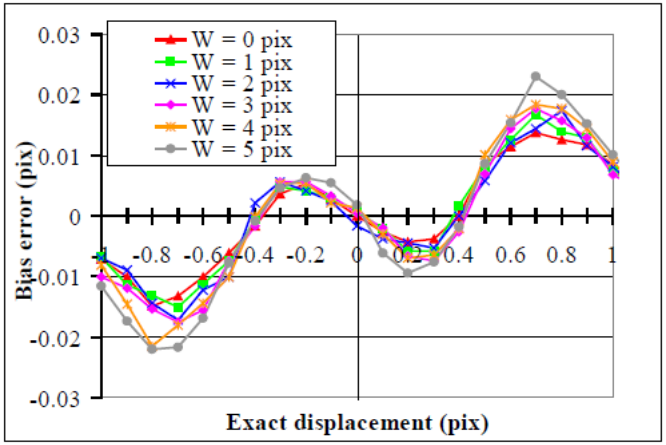

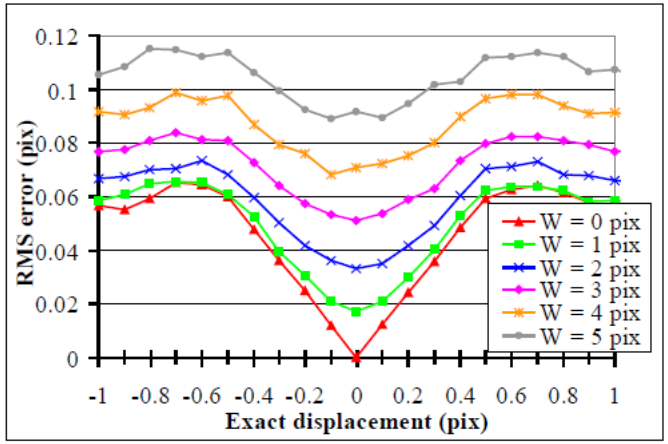

Influence de la 3ème composante

Précision

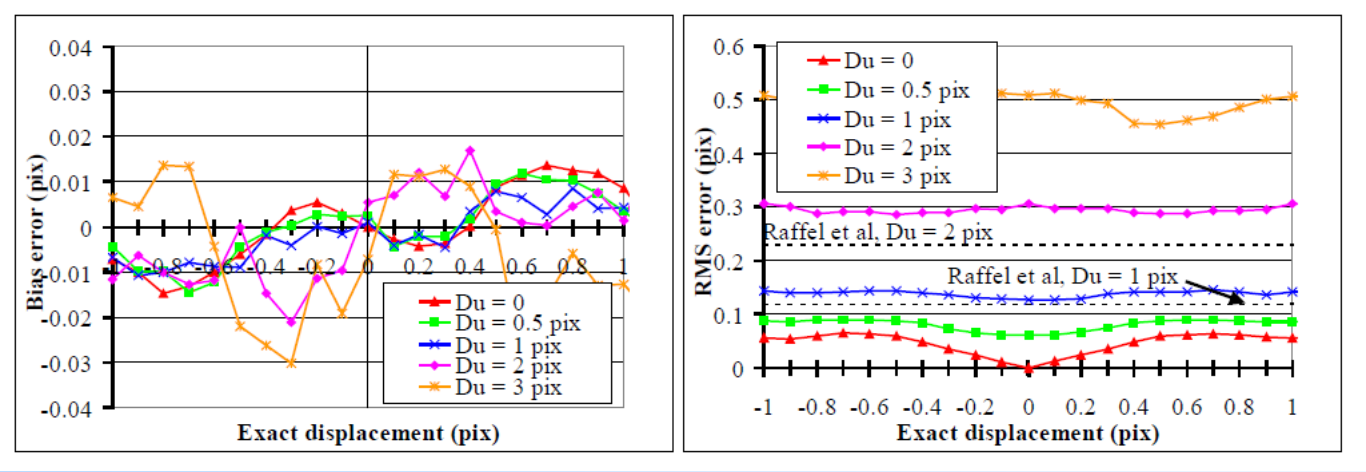

Influence du gradient dans la fenêtre

"Characterization of different PIV algorithms using the Europiv Synthetic Image Generator and real images from turbulent boundary layer." B. MILLIAT, J.M. FOUCAUT, N. PERENNE, M. STANISLAS In Particle Image Velocimetry : proceedings of the EUROPIV 2 open workshop held in Zaragoza on March 31st & April 1st 2003, Springer Verlag, 2004.

Précision

PIV uncertainty quantification by image matching. A. Sciacchitano, B. Wieneke, F. Scarano, Meas. Sci. Technol. 24 (2013)

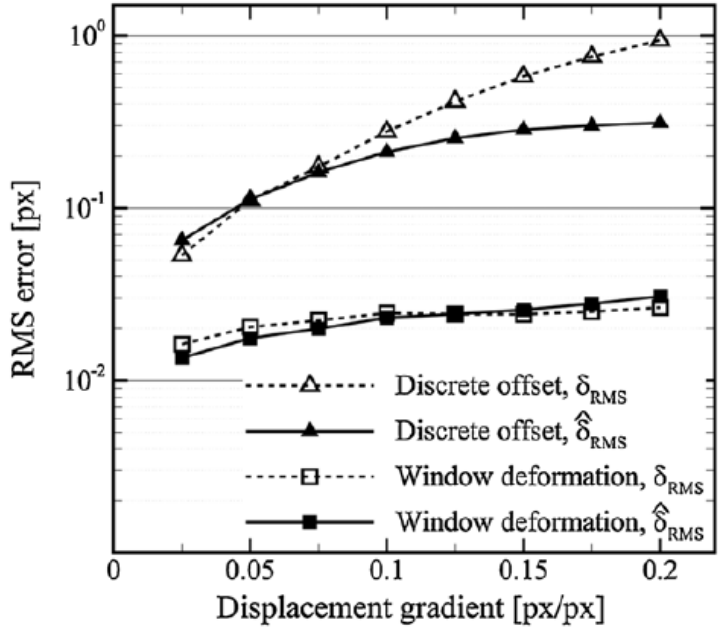

Figure 8. RMS error as a function of the displacement gradient.

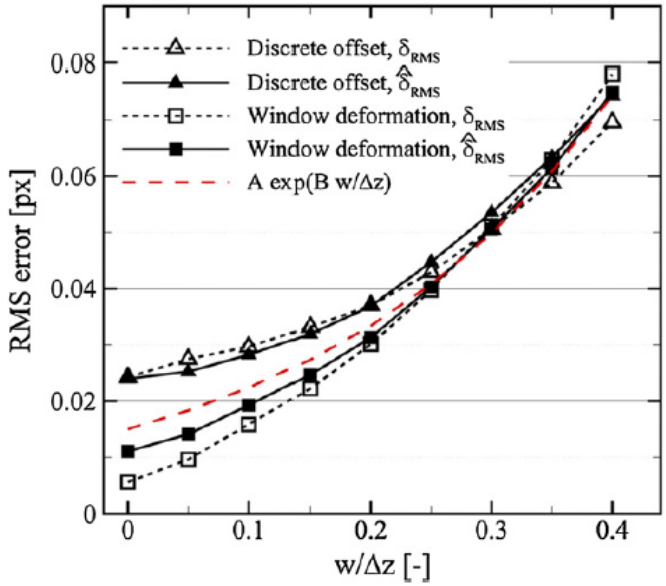

Figure 9. RMS error as a function of the out-of-plane displacement. The red dashed line represents the exponential behavior reported by Nobach and Bodenschatz (2009).

Précision

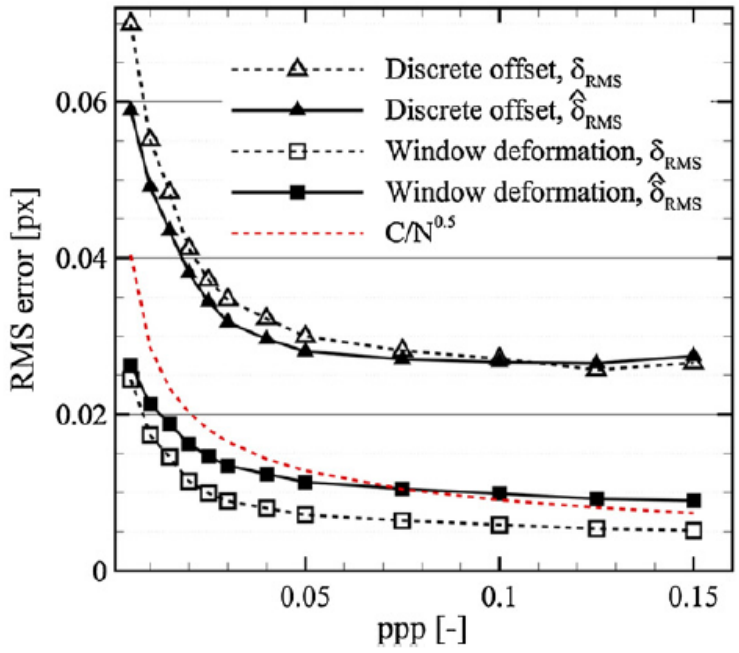

Figure 10. RMS error as a function of the seeding density.

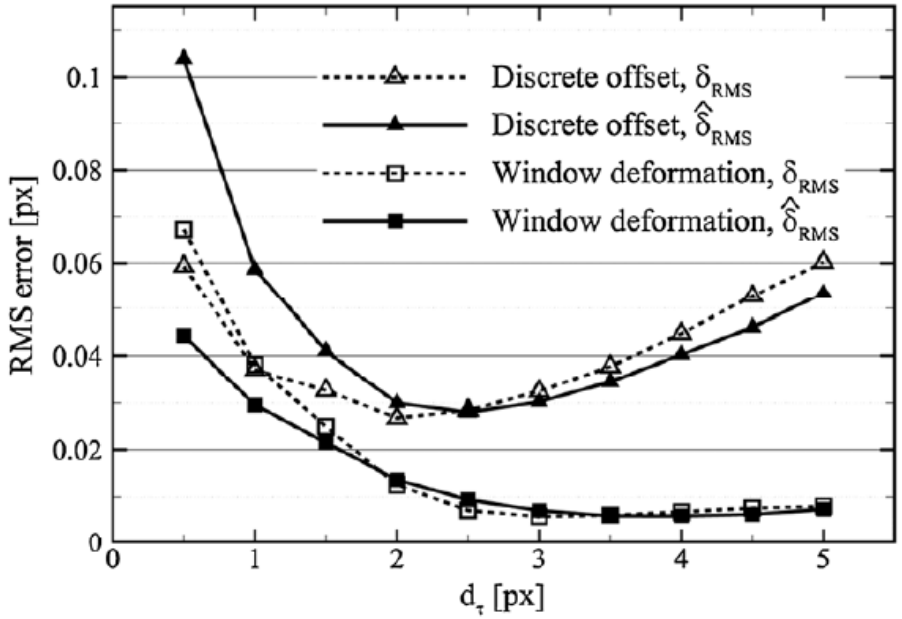

Figure 11. RMS error as a function of the mean particle image diameter.

Précision

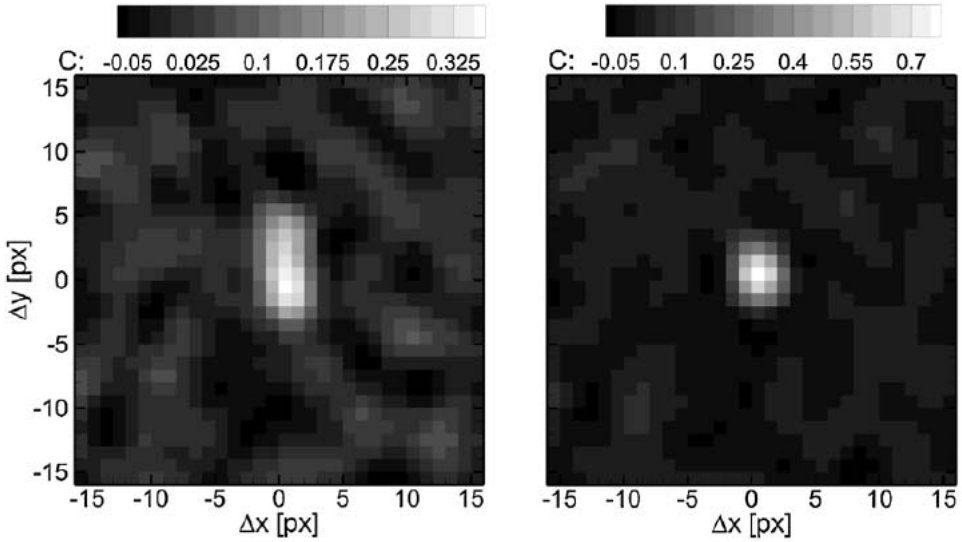

Figure 14. Correlation map along the shear layer (point P1); left: discrete window offset; right: window deformation.

Précision : Turbulence

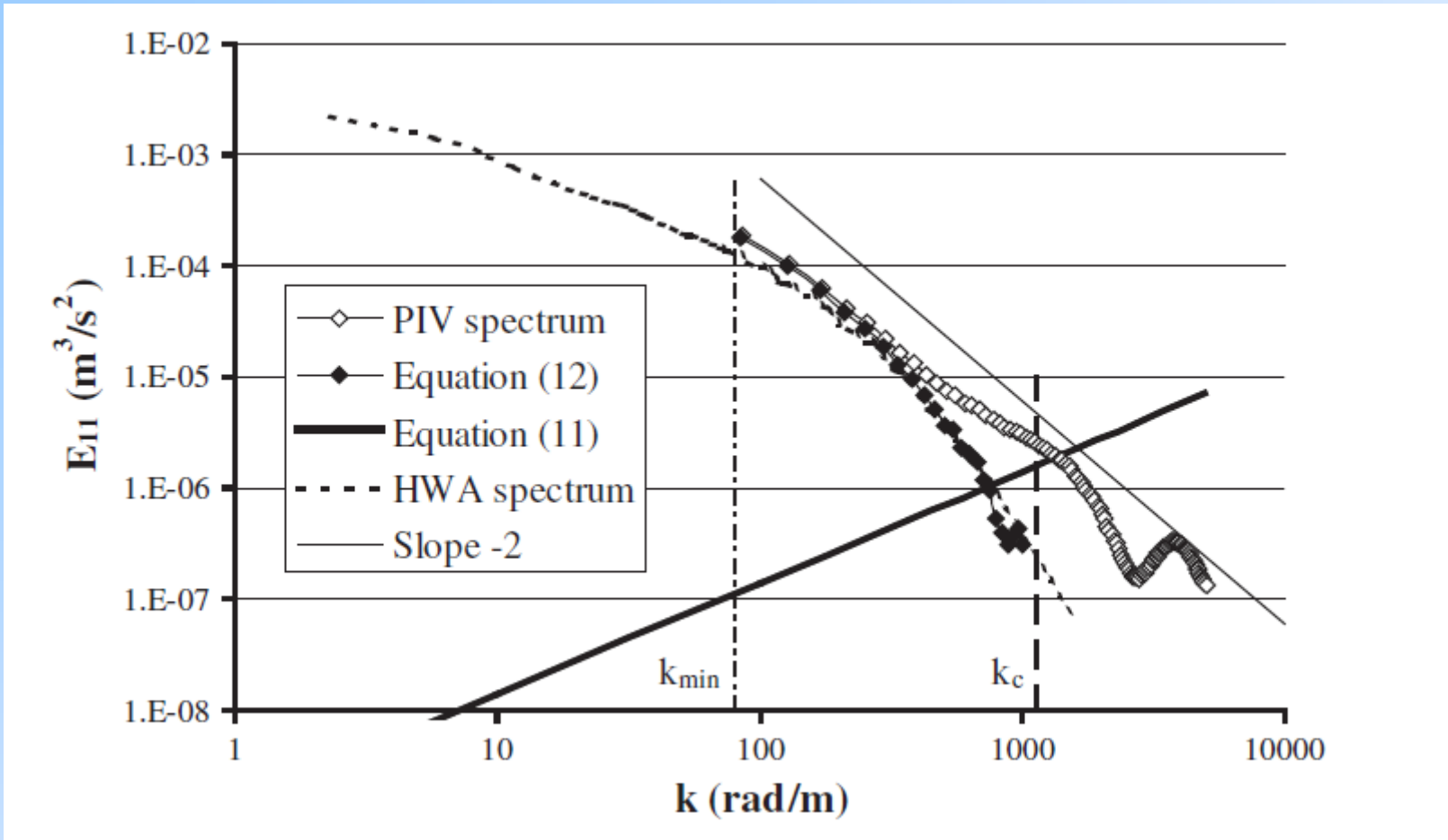

PIV optimization for the study of turbulent flow using spectral analysis
J M Foucaut, J Carlier and M Stanislas, Meas. Sci. Technol. 15 (2004) 1046–1058

Précision

On the uncertainty of digital PIV and PTV near walls. C. J. Kähler, S. Scharnowski, C. Cierpka, Exp Fluids (2012) 52:1641–1656

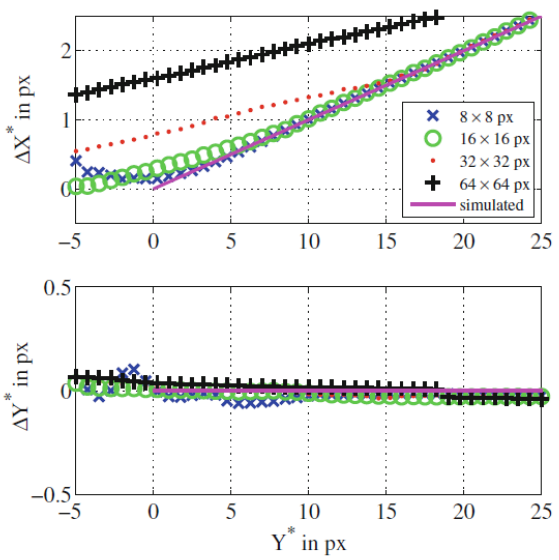

Fig. 2 Estimated displacement profiles for a simulated constant gradient in the near-wall region of a boundary layer using window-correlation for different interrogation windows

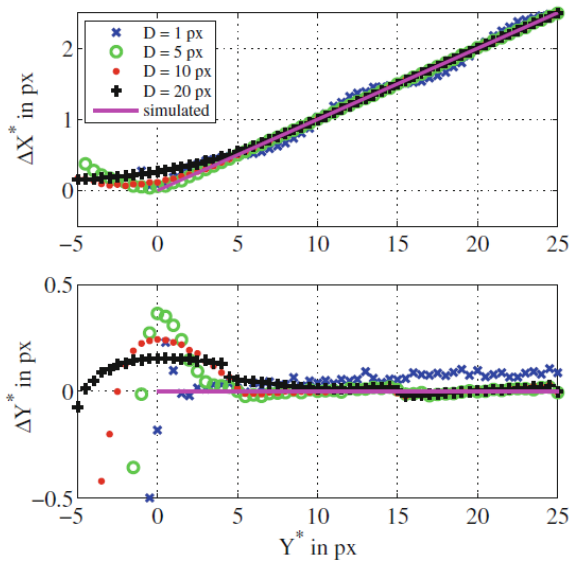

Fig. 3 Estimated displacement profiles for a simulated constant gradient in the near-wall region of a boundary layer using single-pixel ensemble-correlation for different digital particle image diameters

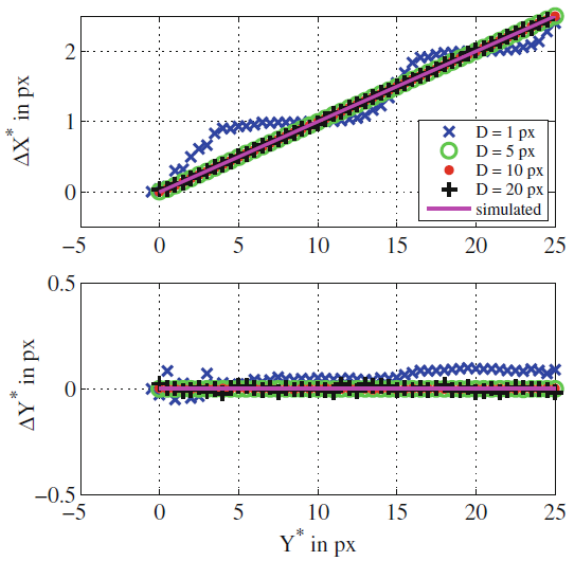

Fig. 8 Estimated displacement profiles for a simulated constant gradient in the near–wall region of a boundary layer using PTV (GC-centroid estimation) for different digital particle image diameters

Window Correlation **Ensemble correlation** **PTV**

Précision

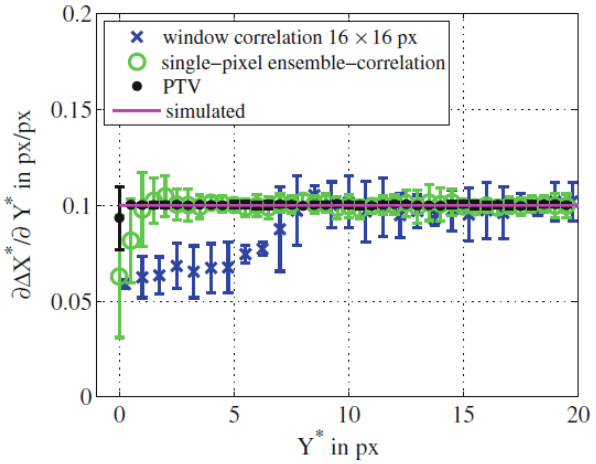

Fig. 10 Profiles of the estimated gradient from Fig. 9 computed using window-correlation, single-pixel ensemble-correlation and PTV

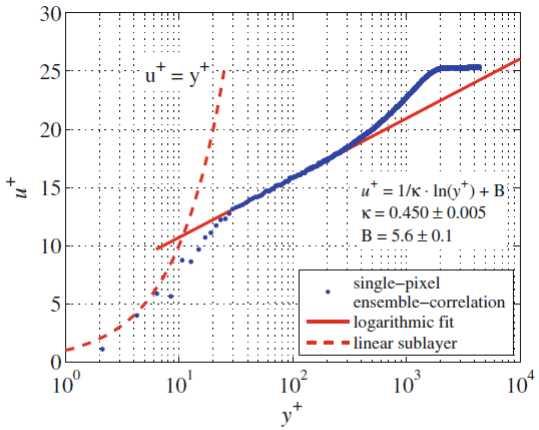

Fig. 12 Velocity profile of the turbulent boundary layer from Fig. 11 normalized with $u_\tau = 0.256$ m/s. The viscous sublayer is not sufficiently resolved. The logarithmic region was approximated by a fit-function

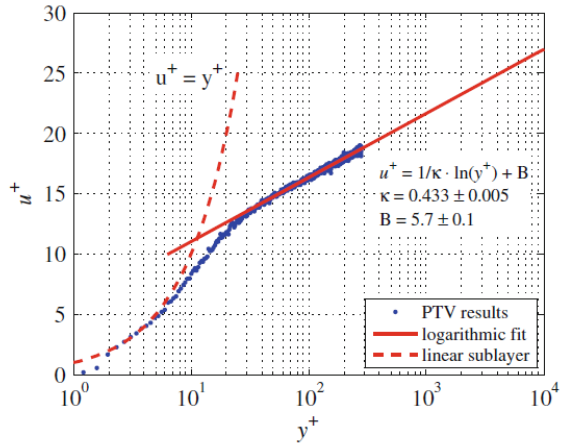

Fig. 14 Normalized velocity profile of a turbulent boundary layer from Fig. 13 normalized with $u_\tau = 0.256$ m/s. The logarithmic region was approximated by a fit-function

gradient de vitesse **Ensemble correlation** **PTV**

- **DSR pour 4000 pixels:**
  - **PIV 16x16 ~ 250**
  - **Correlation d'ensemble ~ 2000**
  - **PTV ~ 25000**
- **PTV : ensemencement inhomogène, gradients non constants, près des parois.**
- **Correlation d'ensemble : pour les grandeurs moyennes**

Précision

Parallax correction for precise near-wall flow investigations using particle imaging. C. Cierpka, S. Scharnowski, and C. J. Kähler, Applied Optics Vol. 52, No. 12 / 2013.

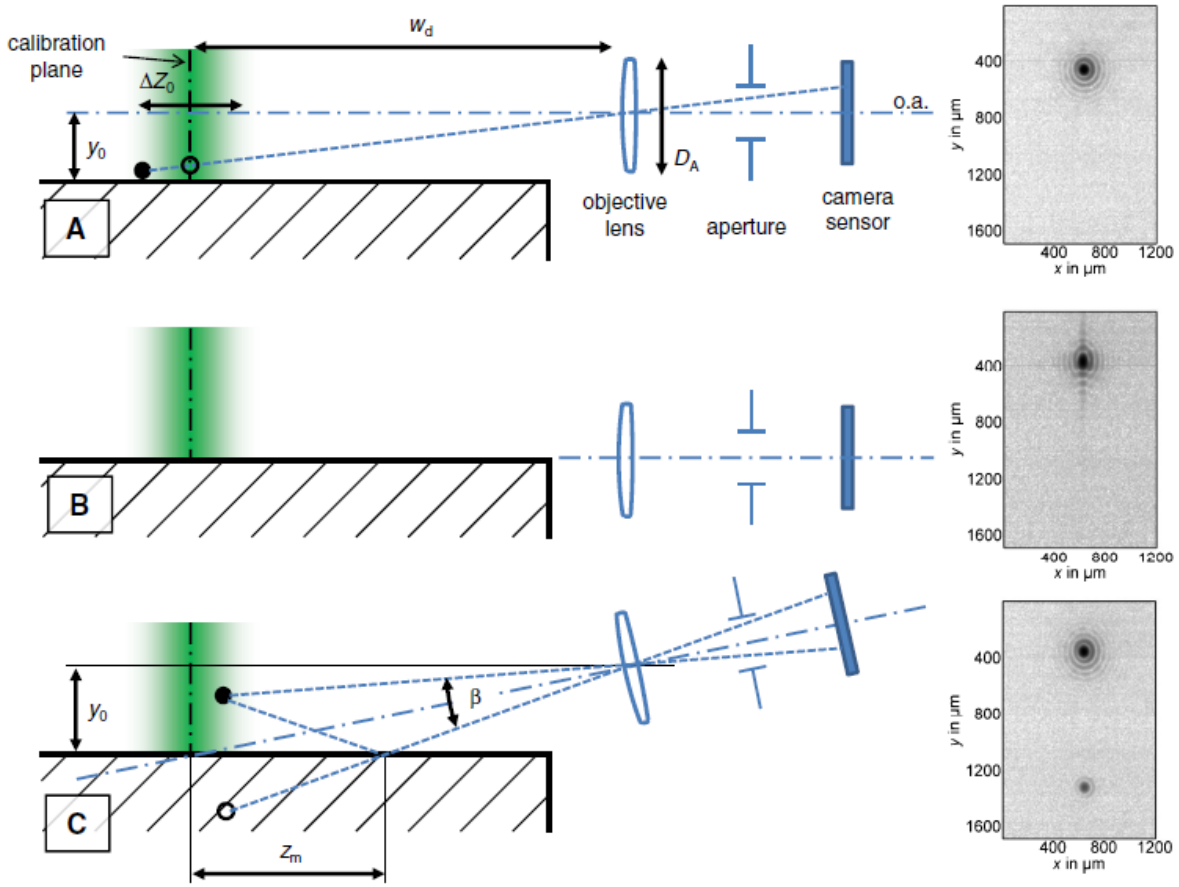

Fig. 1. Different configurations for the near-wall imaging of small particles. (A) objective lens lifted just above the wall, (B) optical axis aligned with the wall, and (C) tilted objective lens (left), not to scale. Corresponding particle image in inverted gray scale (right).

Précision

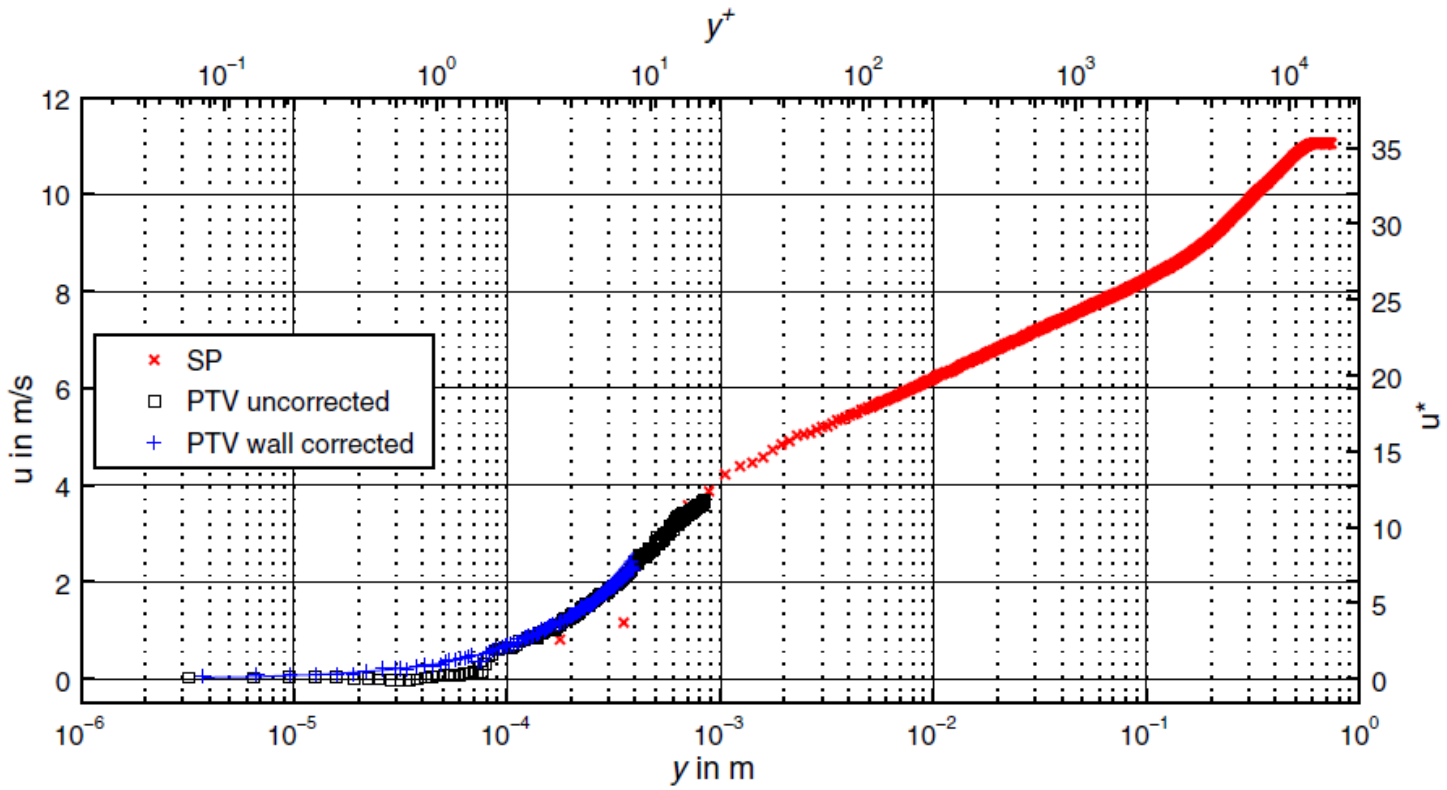

Fig. 8. Normalized velocity profile for the boundary layer at $Re_\delta = 0.4 \times 10^6$, spanning five orders of magnitude for a wall-normal distance ($0.1 < y^+ < 10,000$) with a resolution $\Delta y^+ = 0.08$ of in the near-wall region and $\Delta y^+ = 7.5$ in the outer region.

Précision

PIV uncertainty quantification by image matching. A. Sciacchitano, B. Wieneke, F. Scarano, Meas. Sci. Technol. 24 (2013)

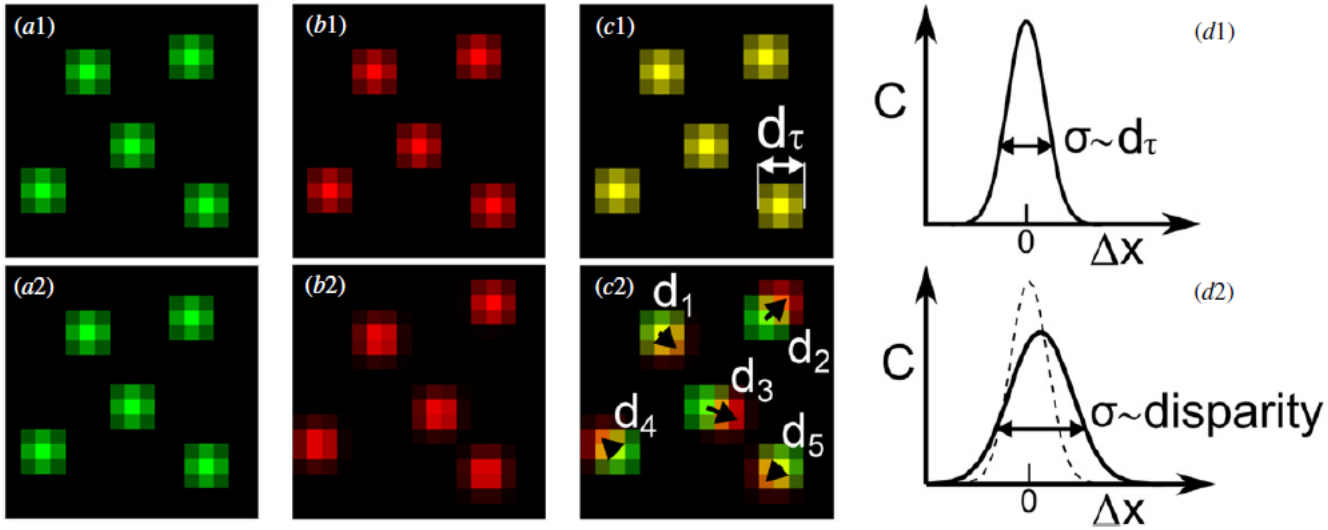

Figure 2. First row: image matching in the ideal case. (*a*1) Particle images of $\widetilde{I}_1$; (*b*1) particle images of $\widetilde{I}_2$; (*c*1) superposition of $\widetilde{I}_1$ and $\widetilde{I}_2$: the green particles of $\widetilde{I}_1$ and the red particles of $\widetilde{I}_2$ superimpose perfectly, yielding the particles displayed in yellow; (*d*1) correlation function (profile) between $\widetilde{I}_1$ and $\widetilde{I}_2$. Second row: image matching in the real case. (*a*2) Particle images of $\widetilde{I}_1$; (*b*2) particle images of $\widetilde{I}_2$; (*c*2) superposition of $\widetilde{I}_1$ and $\widetilde{I}_2$: the particle images do not superimpose perfectly (yellow: particles correctly superimposed; green: portion of $\widetilde{I}_1$ not paired in $\widetilde{I}_2$; red: portion of $\widetilde{I}_2$ not paired in $\widetilde{I}_1$); (*d*2) correlation function (profile) between $\widetilde{I}_1$ and $\widetilde{I}_2$.

Précision

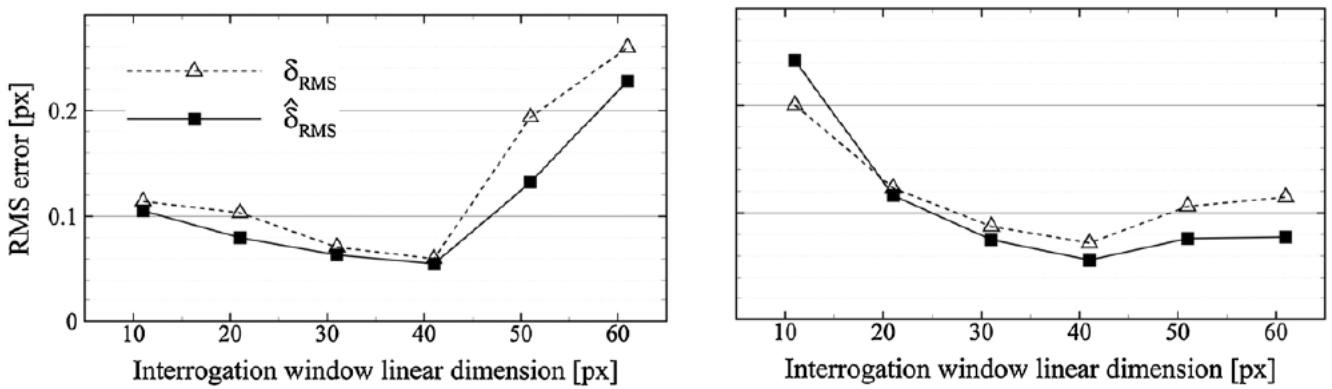

Figure 18. RMS error on the axial velocity component; left: point P1; right: point P2. The symbol key applies to both plots.

Optical set-up

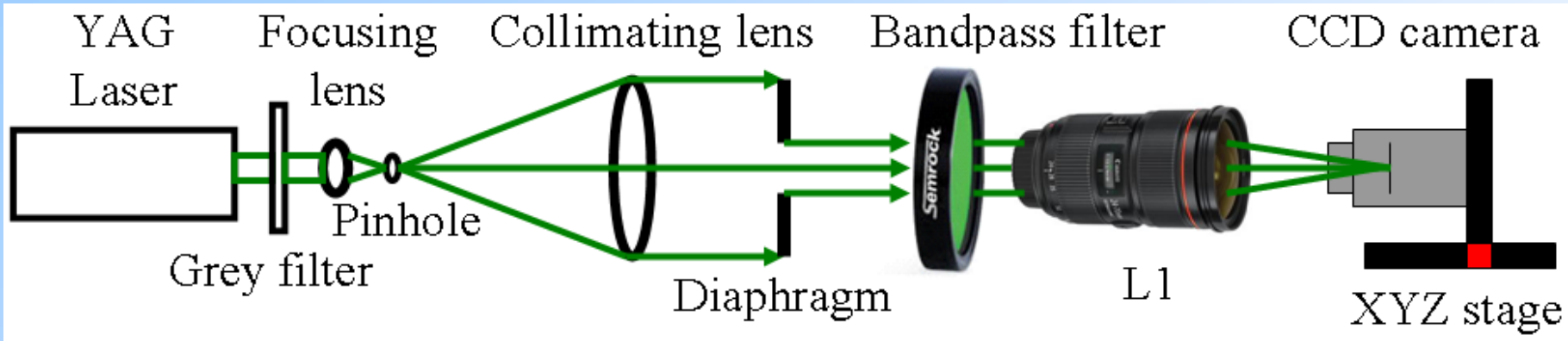

- **Point Spread Function : Edmund Optics MO, f = 20 mm, spotsize = 2.5 μm**
- **Particle simulation : Pentax 67II , f = 105, f# = 2.4, spotsize 2-3 pixels**

PSF & PS scanning

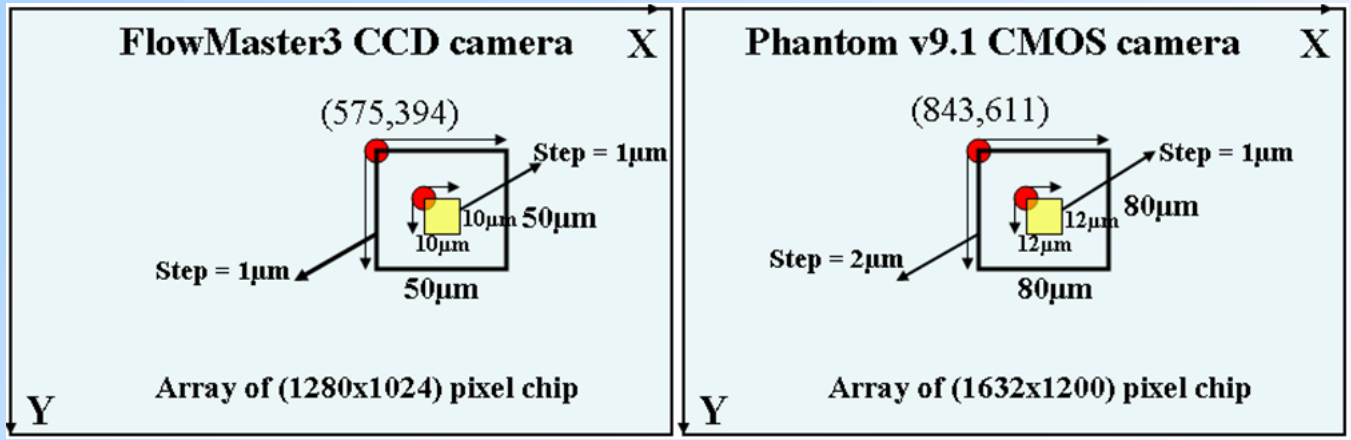

Particle simulation

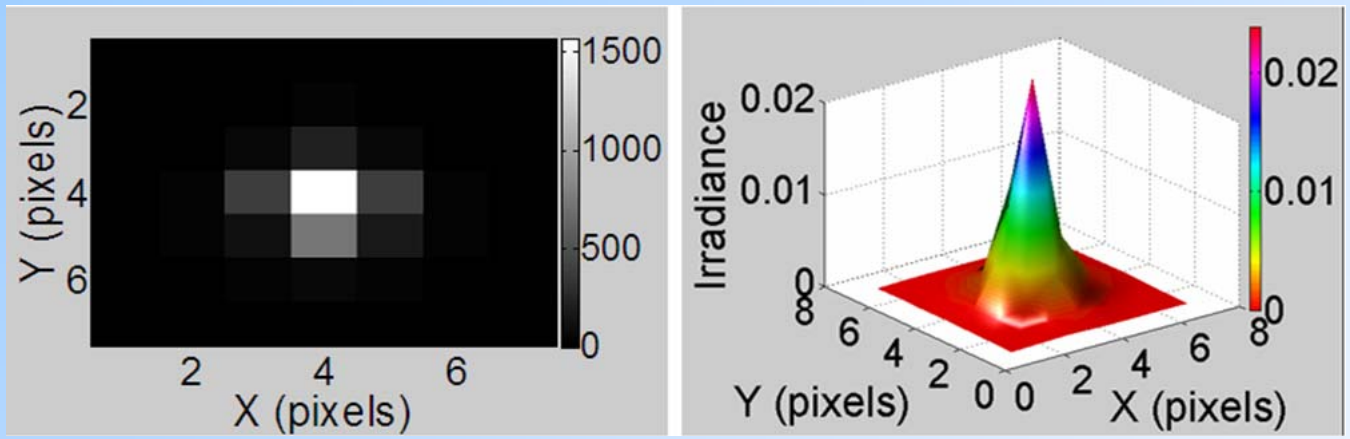

Flowmaster

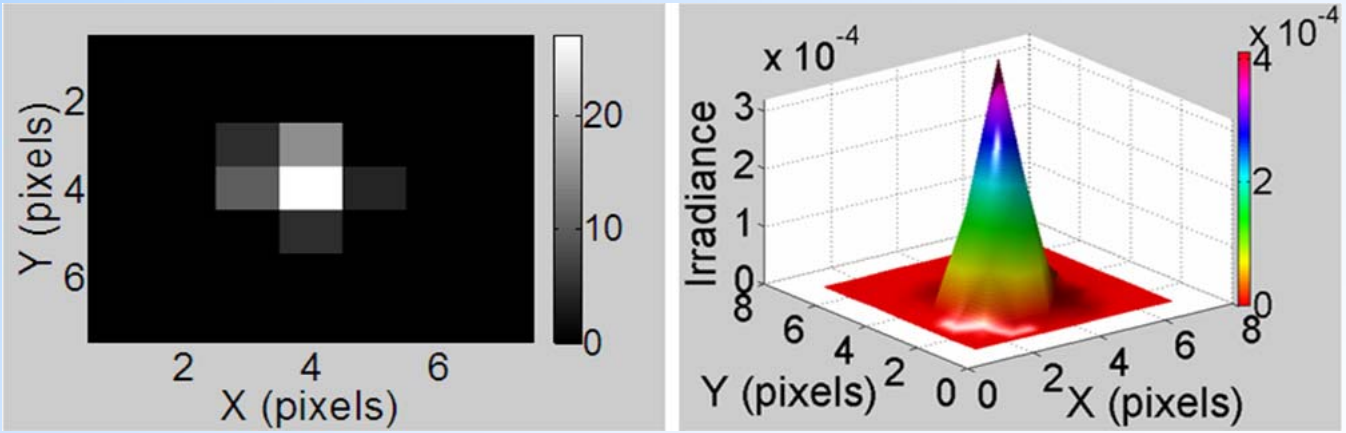

Phantom

Particle displacement simulation

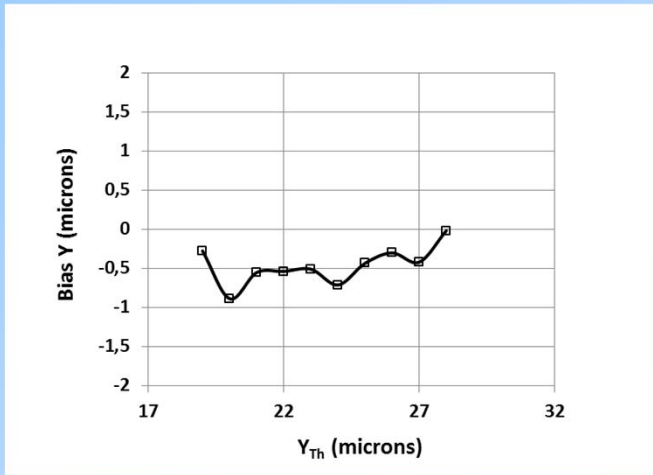

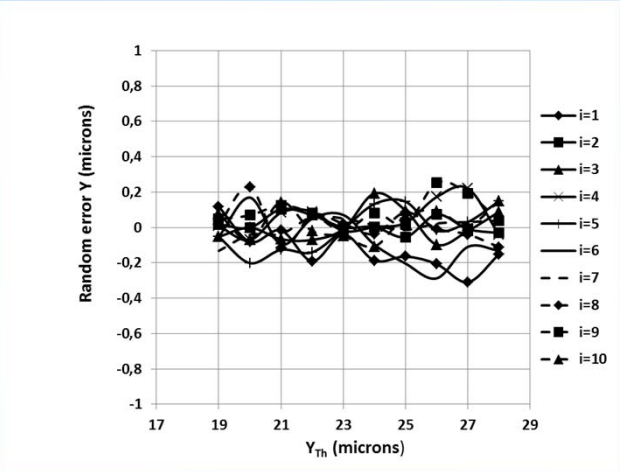

Flowmaster

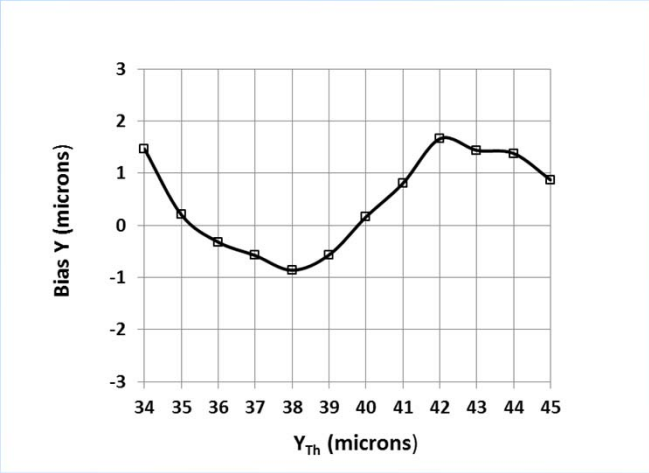

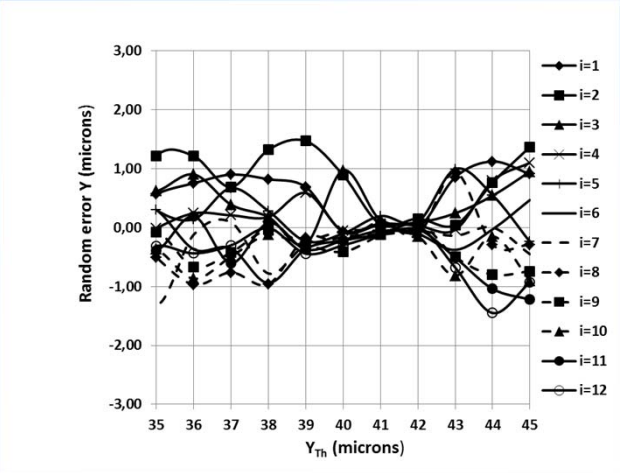

Phantom

Particle displacement simulation

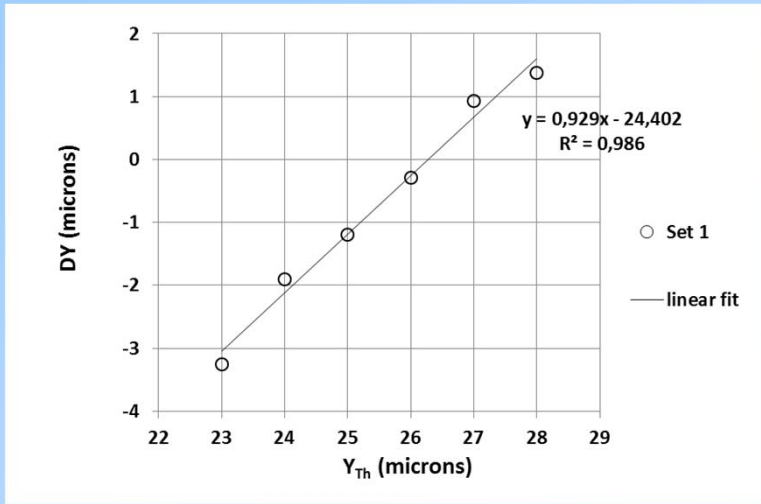

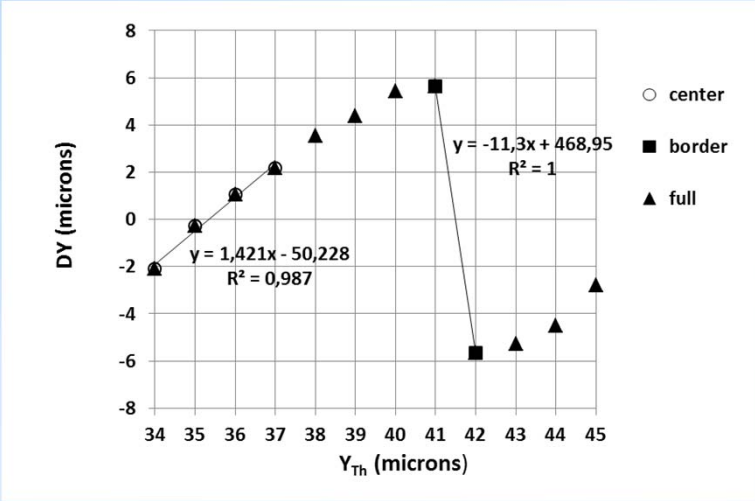

Flowmaster **Phantom**

- **RMS error on position ± 0.03 pix. for Flowmaster**
  ± 0.05 pix. for Phantom

- **Interest of super-resolution PIV**

Résolution spatiale

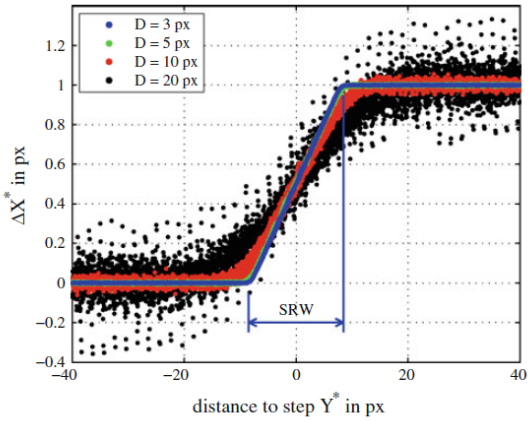

Fig. 8 Response to a step-like velocity profile for different digital particle image sizes computed with window-correlation

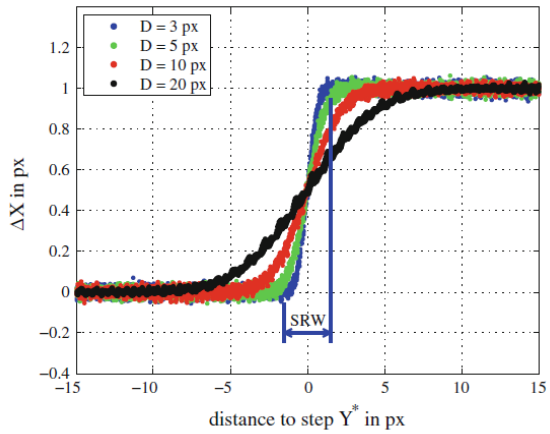

Fig. 9 Response to a step-like displacement profile for different digital particle image sizes computed with single-pixel ensemble-correlation

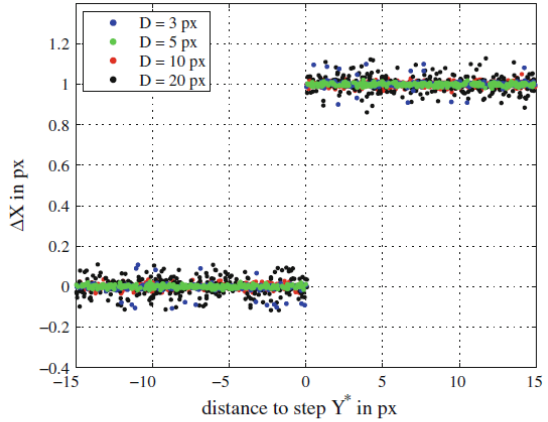

Fig. 10 Response to a step-like displacement profile for different digital particle image sizes computed with PTV algorithms

Réponse à un échelon de vitesse

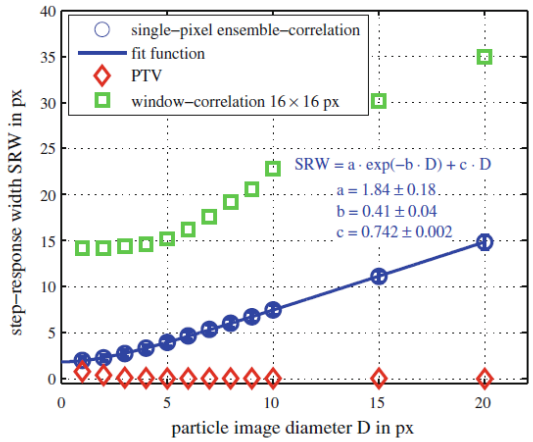

Fig. 11 Step response width of the estimated displacement with respect to the digital particle image diameter

On the resolution limit of digital particle image velocimetry. C. J. Kähler, S. Scharnowski , C. Cierpka, Exp Fluids (2012) 52:1629–1639

3D3C

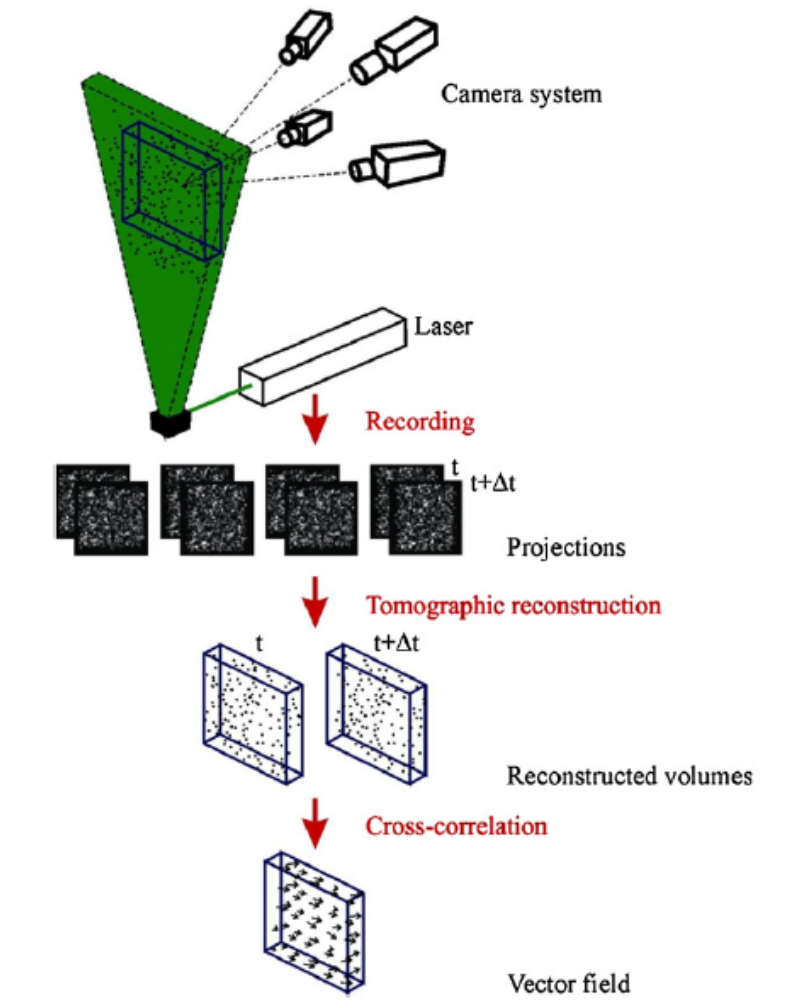

Figure 3. Working principle of tomographic PIV (reproduced from Elsinga *et al* 2005a).

Tomographic PIV: principles and practice, F Scarano, Meas. Sci. Technol. 24 (2013)

3D3C

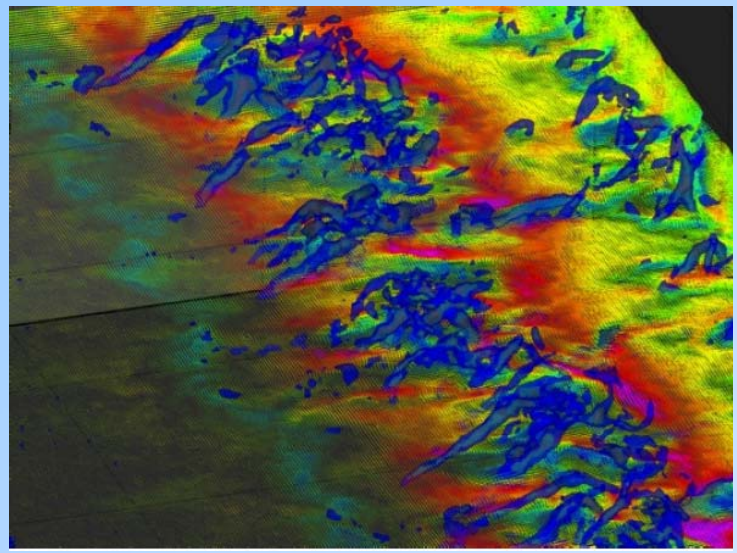

High-res backward facing step

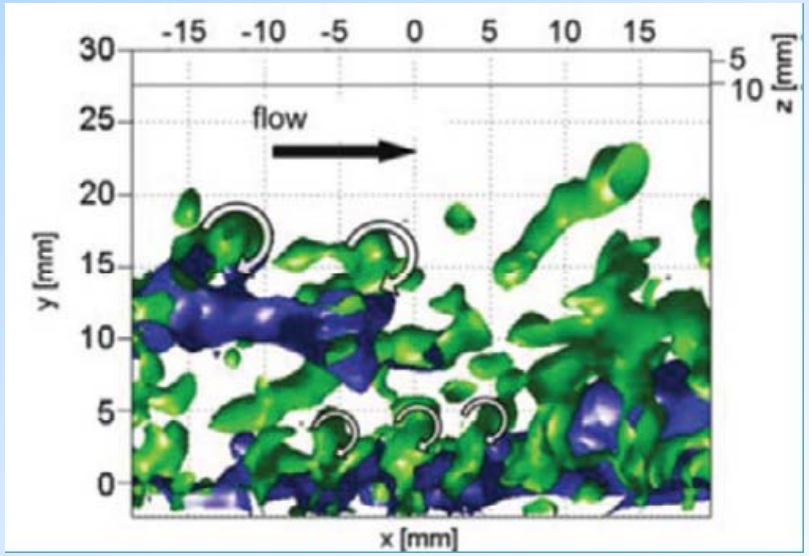

Low speed turbulent boundary layer

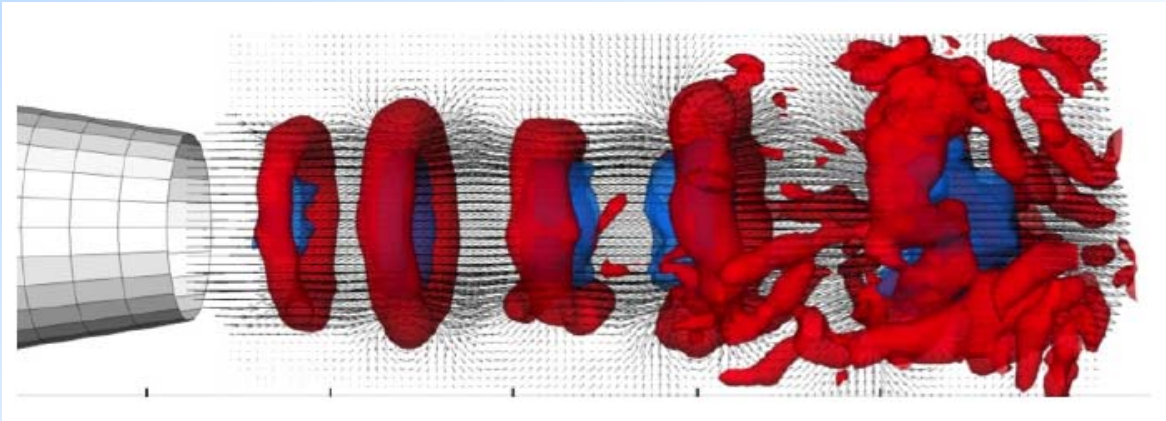

Transitional jet

3D3C

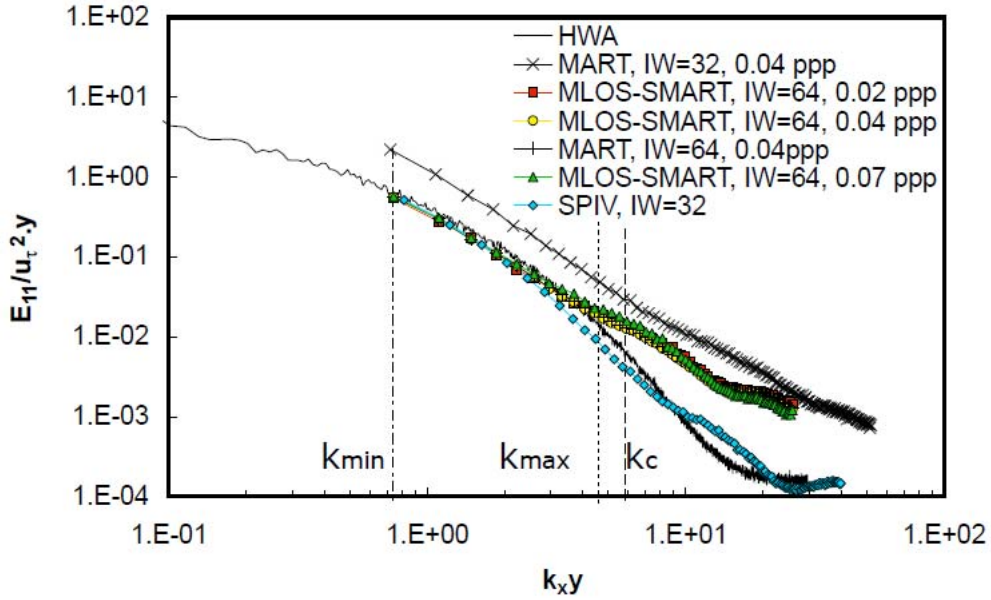

Figure 4.29: Longitudinal velocity power spectra for the $1200 \times 180 \times 1200$ point volume TPIV at $\mathrm{Re}_\theta = 7800$, $y^+ = 53$. SPIV $IW = 32^2$ px with 75% region overlap. A hot-wire derived spectra is shown for comparison.

TRPIV

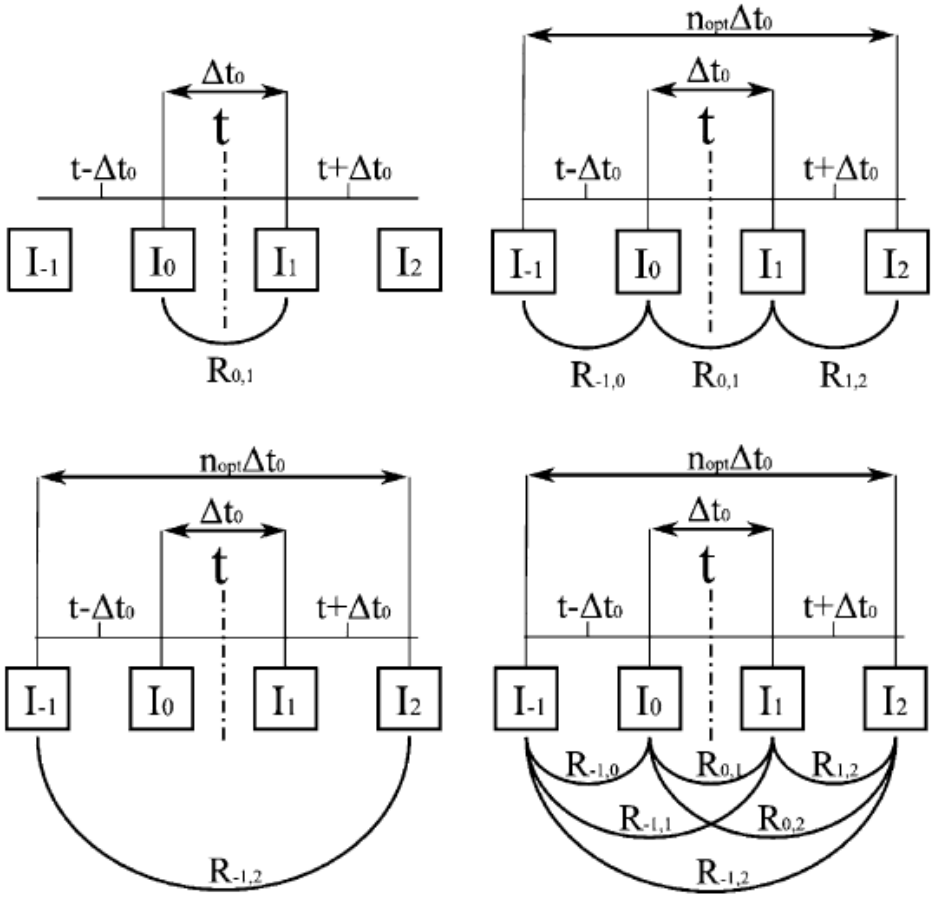

Fig. 6 Schemes of the techniques: SP-cΔt (*top-left*), EC-cΔt (*top-right*), SP-aΔt (*bottom-left*), *pyramid correlation* (*bottom-right*)

TRPIV

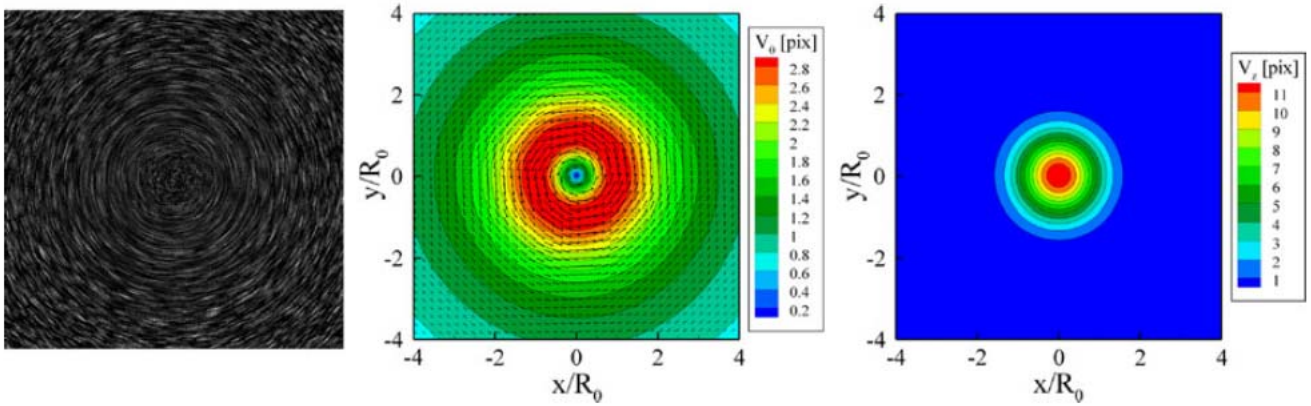

Fig. 5 3D vortex simulation: overlay of 10 subsequent images (*left*), exact tangential velocity (*center*) and axial velocity (*right*)

Fig. 7 Mean bias error (*left*) and root-mean-square error (*right*) on the horizontal displacement; **a** SP-cΔt; **b** EC-cΔt; **c** SP-aΔt; **d** *pyramid correlation*

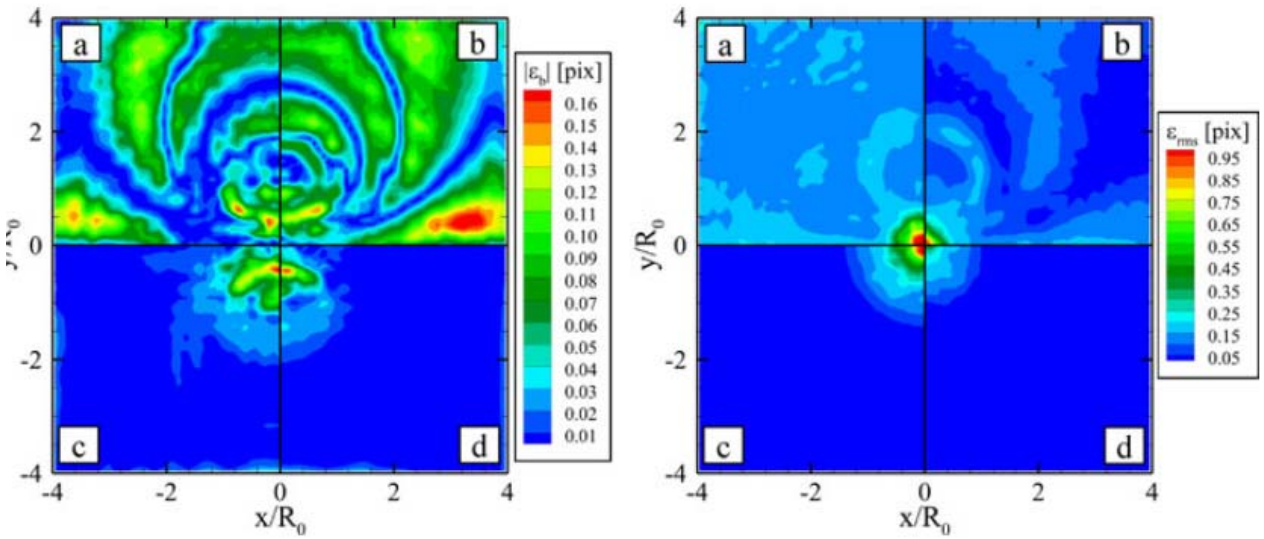

Conclusion

- **Ca bouge!**
- **Il faut savoir ce que l'on veut…**
- **4ème Challenge international de PIV Lisbonne juillet 2014**